International Journal of Engineering Research and Modern Education (IJERME)
Impact Factor: 7.018, ISSN (Online): 2455 - 4200
(www.rdmodernresearch.com) Volume 7, Issue 2, 2022

COMPUTATIONAL ANALYSIS OF A CORRUGATED DRAGONFLY AIRFOIL AT LOW REYNOLDS NUMBER

R. Rajesh Kumar*, K. Arun Prasath, K. Gurunath***, L. Harirama Krishnan**** & S. Rajkumar*****
Department of Aeronautical Engineering, Dhanalakshmi Srinivasan Engineering College, Perambalur, Tamil Nadu

Cite This Article: R. Rajesh Kumar, K. Arun Prasath, K. Gurunath, L. Harirama Krishnan & S. Rajkumar, "Computational Analysis of a Corrugated Dragonfly Airfoil at Low Reynolds Number", International Journal of Engineering Research and Modern Education, Volume 7, Issue 2, Page Number 61-69, 2022.

Abstract:

The chord Reynolds number of micro air vehicles are usually in the range of 104 to 105. The laminar flow separation is a common phenomenon occurring in a flow over a body. The corrugated dragonfly airfoil has the potential ability to sustain an attached flow at low Reynolds number, thereby suppressing laminar flow separation or large laminar bubbles. In this project an optimized corrugated dragonfly airfoil is designed from the survey of standard airfoils. The flow properties of the corrugated dragonfly airfoil are measured at different angles of attack such as 0º, 5º, 10º and 15º for the Reynolds number of 5×104 in which the MAVs usually operates. The aerodynamic performance of corrugated dragonfly airfoil is compared with a traditional NACA 0012 airfoil at the same Re and also with a corrugated dragonfly airfoil at a different Re of 34000. The corrugated airfoil is meshed using GAMBIT and the computational fluid flow analysis is carried out using FLUENT on the corrugated dragonfly airfoil at low Reynolds number of 5×104. The flow behavior around the airfoil is analyzed and simulations are carried out to predict the behavior of unsteady flow structures around the airfoil at different angles of attack.

Introduction:

MICRO-Air-Vehicles (MAVs), which typically refer to palm-sized aircraft (e.g. with a maximum dimension about 10cm and a flight speed about 10m/s), are of great interest to both military and civilian applications. Equipped with video cameras, transmitters or sensors, these miniaturized aerial vehicles can perform surveillance, reconnaissance, targeting, or bio-chemical sensing tasks at remote, hazardous or dangerous locations. A concerted effort supported by the Defense Advanced Research Projects Agency (DARPA) in recent years has resulted in advancements in miniaturized digital electronics, micro fabrication, miniaturized power cells, remote communication, imaging and control devices and other enabling technologies. Such advances have turned the concept of MAVs as rapidly deployable eyes-in-the-sky from fiction into demonstrated facts. The continuing demand for such small and robust miniaturized aerial vehicles is making MAVs an emerging sector of the aerospace market, and MAVs are expected to become commonplace in the next ten to twenty years.

Methodology:

Computing unsteady flows at low to moderate Reynolds numbers continues to be of significant interest due to its application in MAVs and its relevance to insect and bird flights. Flapping and hovering flight of bird and insect are fine examples of optimum motion of aerodynamic surfaces that simultaneously develop necessary thrust for forward motion and sustained lift to keep it airborne. This is totally different from aircraft motion where lift and thrust are created by different sub-systems. Also, lift and thrust are created in aircraft by steady flow devices, while natural fliers use unsteady aerodynamics to create the same by articulating same surfaces.

Design:

The process of airfoil design proceeds from a knowledge of the boundary layer properties and the relation between geometry and pressure distribution. The goal of an airfoil design varies. Some airfoils are designed to produce low drag (and may not be required to generate lift at all.) Some sections may need to produce low drag while producing a given amount of lift. In some cases, the drag doesn't really matter but it is maximum lift that is important. The section may be required to achieve this performance with a constraint on thickness, or pitching moment, or off-design performance, or other unusual constraints.

One approach to airfoil design is to use an airfoil that was already designed by someone who knew what he or she was doing. This design by authority works well when the goals of a particular design problem happen to coincide with the goals of the original airfoil design. This is rarely the case, although sometimes existing airfoils are good enough. In these cases, airfoils may be chosen from catalogs such as Selig's Airfoils at Low Speeds. The advantage to this approach is that there is test data available. No surprises, such as an unexpected early stall, are likely. On the other hand, available tools are now sufficiently refined that one can be

reasonably sure that the predicted performance can be achieved. The use of designer airfoils specifically tailored to the needs of a given project is now very common.

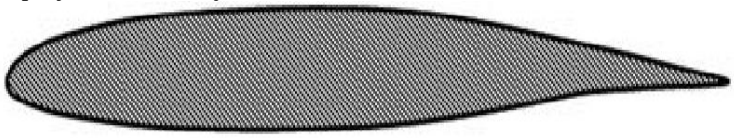

Figure 1: Streamlined GA (W) - 1 Airfoil

Design Limitation:

The common problems occurs during an airfoil design are

- Design for maximum thickness
- Design for maximum lift
- Laminar boundary layer airfoil design
- High lift or thickness transonic design
- Low Reynolds number airfoil design
- Low or positive pitching moment designs
- Multiple design points

Design of Corrugated Dragonfly Airfoil:

The corrugated dragonfly airfoil is designed using GAMBIT software. The constraints for designing the airfoil are taken from the journal Computational Study of Unsteady Flows around Dragonfly and Smooth Airfoils at Low Reynolds Numbers by H. Gao, Hui Hu, Z. J. Wang. The dimensions are shown in the below figure.

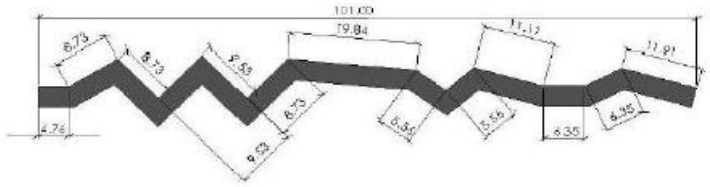

Figure 2: Dimensions of Corrugated Dragonfly Airfoil

The cross section of the bio-inspired corrugated airfoil corresponds to a typical cross section of a dragonfly wing, which was digitally extracted from the profile given in Vargas and Mittal. The maximum effective thickness of the corrugated airfoil (i.e., the airfoil shape formed by fitting a spline through the protruding corners of the corrugated cross section) is about 15% of the chord length, which is slightly smaller than that of the streamlined GA(W)-1 airfoil (17% of the chord length). The bio inspired corrugated airfoil has the chord length of C=100 cm. The schematic diagram of the corrugated dragonfly airfoil designed using GAMBIT software is shown below.

Figure 3: Designed Corrugated Dragonfly Airfoil

Design constraints

- Chord length = 100 mm
- Thickness = 5 m

Meshing:

In order to conduct a CFD analysis, three main tasks must be completed: grid generation, or pre-processing, the actual computational processing of the analysis, and visualization of the computational results, or post-processing. As CFD matured over the past few decades, each of these steps has become a discipline in and of itself.

Grid Generation:

Grid generation is done with the help of gambit software. Before CFD can be used to calculate the aerodynamic characteristics of a flow, the physical space through which the flow passes must be divided into a

number of discrete points, forming a grid. The grid must then be transformed from the physical domain into a computational domain, which is a form that the flow solver program understands and uses to perform the numerical calculations described below. This transformation between the physical and computational domain can be accomplished by using commercially available software, such as GridGen or GAMBIT. These programs take in a computer-aided design model of the flight vehicle, and with guidance from the user for details such as grid type and resolution, build the physical grid, which is then transformed into a computational grid ready for use with the flow solver.

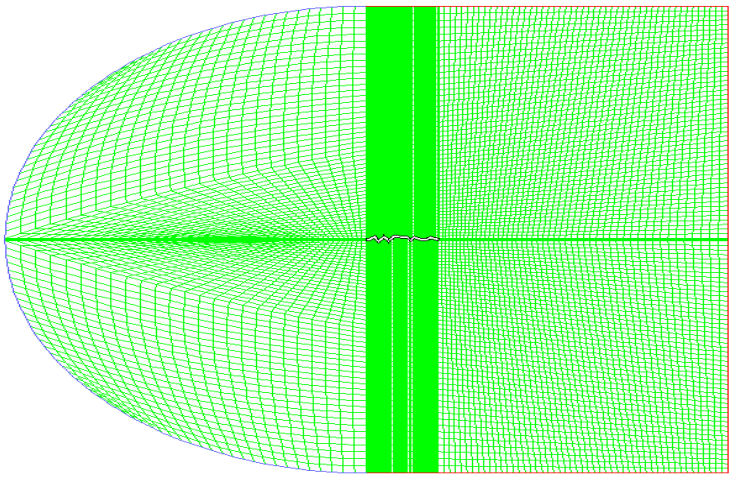

Figure 4: Grid System for Corrugated Dragonfly Airfoil

Computational Fluid Dynamics:

Computational fluid dynamic (CFD) analysis is a powerful, cost-effective tool for the study of the aerodynamic characteristics of a flow. Through careful selection of the grid geometry and resolution, as well as the computational technique used, the sophistication of the analysis can be tailored to meet the needs of the researcher, while conforming to the imposed time and cost constraints. Today, CFD finds extensive usage in basic and applied research, in design of engineering equipment, and in calculation of environmental and geophysical phenomena. Since the early 1970s, commercial software packages (or computer codes) became available, making CFD an important component of engineering practise in industrial, defence, and environmental organizations.

Governing Equation Using In CFD:

- Continuity equation
- Momentum equation
- Energy equation

The CFD Analysis Process:

In order to conduct a CFD analysis, three main tasks must be completed: grid generation, or pre-processing, the actual computational processing of the analysis, and visualization of the computational results, or post-processing. As CFD matured over the past few decades, each of these steps has become a discipline in and of itself.

Performance Analysis:

In the present study computational tests were carried out to get an understanding of the flow characteristics over a corrugated dragonfly aerofoil at a Reynolds number of 5×104 and at a velocity of 7.3 m/s. structured meshes have been used for depicting the motion of fluid over the aerofoil. First a grid has been selected after conducting a grid study. Two dimensional simulations were carried out with standard SST k-ω model using FLUENT. Computational results are compared with the data available for corrugational dragonfly aerofoil at a Reynolds number of 34,000 and NACA 0012 aerofoil at same Reynolds number of 5×104. The results obtained from the computational tests revealed the increased performance of the corrugated dragonfly aerofoil at Re of 5×104 over the other which are compared.

Model for Analysis:

Based on the literature study carried out, the corrugated dragonfly aerofoil was found to have the highest aerodynamic performance at low Reynolds number. The schematic model of the traditional streamlined NACA 0012 aerofoil taken for comparing the performance of the corrugated dragonfly aerofoil is shown in the following figure. The aerodynamic performance characteristics of this aerofoil are taken from the base paper studied in the literature survey. The designed NACA 0012 aerofoil using the co-ordinates obtained is shown in the below figure. NACA 0012 aerofoil is a symmetric aerofoil used for low speed applications. Hence this aerofoil model is used for comparing the performance of corrugated dragonfly aerofoil.

Figure 5: NACA 0012 Aerofoil

The corrugated dragonfly aerofoil is designed using GAMBIT software using the measured design constraints. The schematic diagram of the designed corrugated dragonfly aerofoil is shown in the below figure.

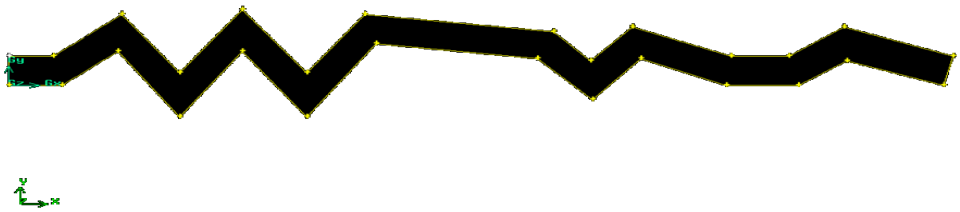

Figure 6: Corrugated Dragonfly Airfoil

Performance Measure:

The results of the flow analysis over the corrugated dragonfly aerofoil are revealed and measured after the solver converge the solution. The pressure and velocity contours of different angle of attack are plotted.

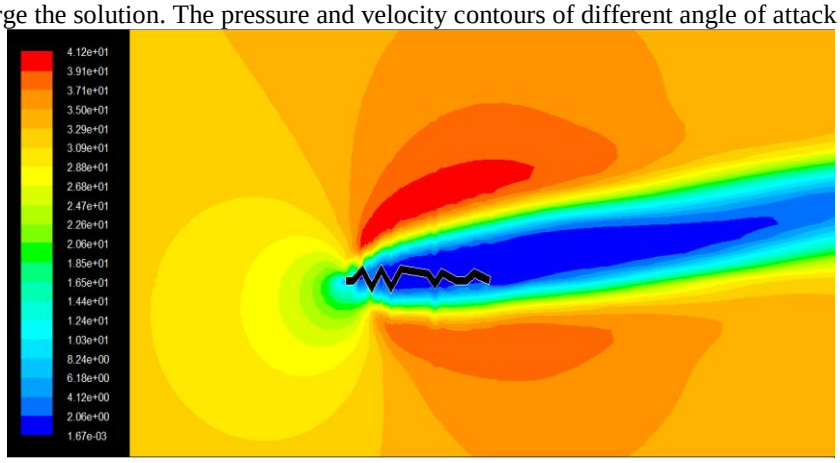

Figure 7: Contour of Dynamic Pressure At 10º AOA

- Contour of dynamic pressure at 0º AOA (Appendix G.1)
- Contour of dynamic pressure at 5º AOA (Appendix G.2)
- Contour of dynamic pressure at 15º AOA (Appendix G.3)

From all these contour diagram of dynamic pressures at different angles of attack, it is clear that the pressure difference between the upper and the lower surface is greater at 15 degrees of angle of attack. The greater the pressure difference, the greater the lift since every object moves from higher pressure to lower pressure. Therefore maximum lift can be obtained at this angle of attack.

This can be shown more clearly by plotting the pressure co-efficient contours at different angles of attack.

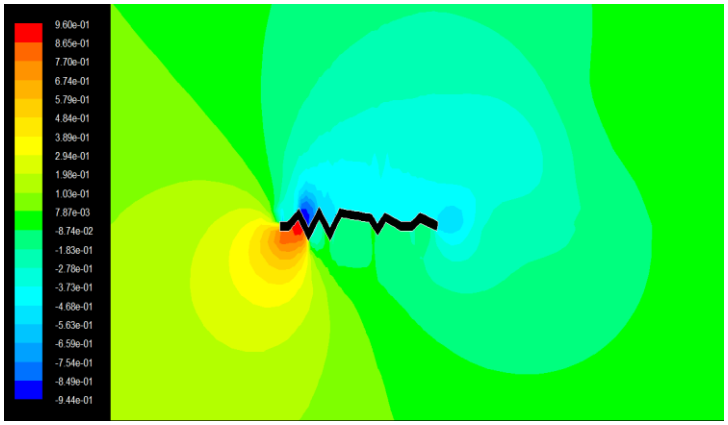

Figure 8: Contour of Pressure Co-Efficient At 15º AOA

- Contour of pressure co-efficient at 0º AOA (Appendix G.4)
- Contour of pressure co-efficient at 5º AOA (Appendix G.5)
- Contour of pressure co-efficient at 10º AOA (Appendix G.6)

The velocity contours shows the variation of velocity along the surface of the corrugated dragonfly aerofoil. At 0 degree angle of attack, the velocity distribution of air on both sides of the aerofoil is found to be the same. The variation of velocity distribution increases as the angle of attack increases. At 15 degree angle of attack, the velocity distribution on the upper aerofoil surface is seen to be more varied from the lower surface. It can be understood from the velocity magnitude contour diagram shown below.

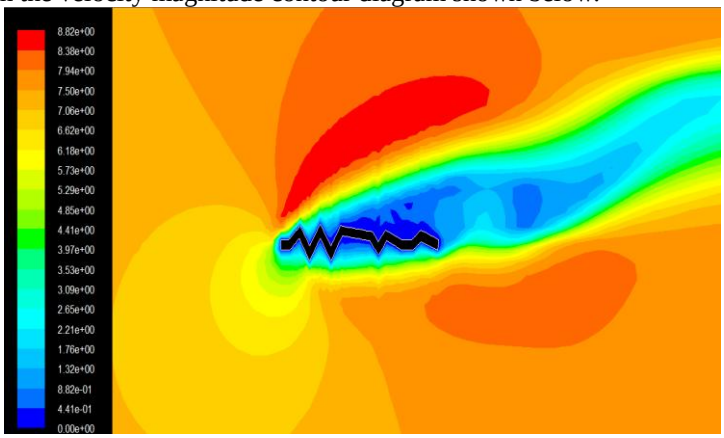

Figure 9: Contour of Velocity Magnitude at 15º AOA

- Contour of velocity magnitude at 0º AOA (Appendix G.7)
- Contour of velocity magnitude at 5º AOA (Appendix G.8)
- Contour of velocity magnitude at 10º AOA (Appendix G.9)

The direction of flow over the corrugated dragonfly aerofoil is shown in the velocity vector contour. At 0º angle of attack, the flow direction is same at all the points. As the angle of attack increases from 5º to 15º, the reversed flow is formed on the upper surface of the aerofoil. The contours of velocity vector at different angle of attack are shown below.

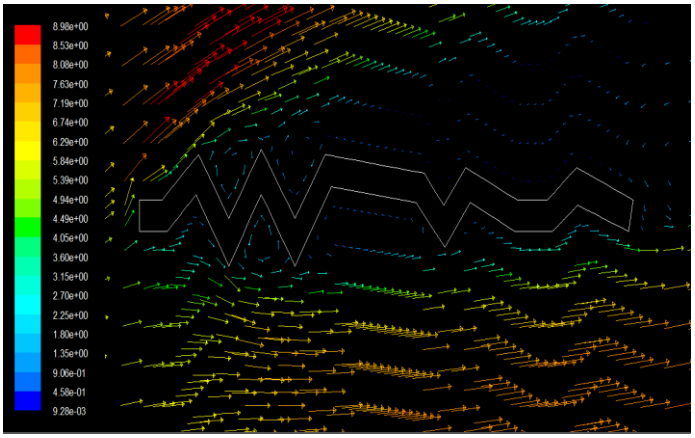

Figure 10: Velocity Vector Contour At 15º AOA

- Contour of velocity vector at 0º AOA (Appendix G.10)
- Contour of velocity vector at 5º AOA (Appendix G.11)
- Contour of velocity vector at 10º AOA (Appendix G.12)

These velocity vector contours clearly shows the direction of flow over the corrugated dragonfly aerofoil at different angles of attack.

Performance Analysis:

The co-efficient of pressure (Cp) is plotted for different angle of attack along the chord length. At large angle of attack, the co-efficient of pressure between the upper and lower aerofoil surface is greater and it increases till the stalling angle. The co-efficient of pressure plots for different angle of attack is shown below.

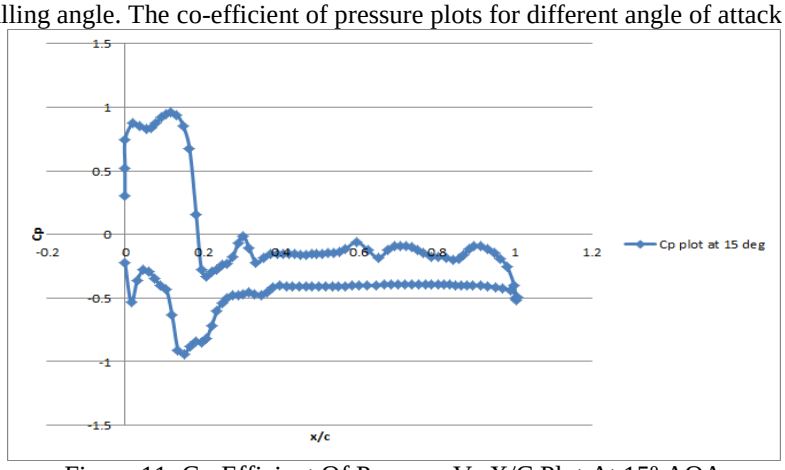

Figure 11: Co-Efficient Of Pressure Vs X/C Plot At 15º AOA

- Co-efficient of pressure vs x/c plot at 0º AOA (Appendix G.13)
- Co-efficient of pressure vs x/c plot at 5º AOA (Appendix G.14)
- Co-efficient of pressure vs x/c plot at 10º AOA (Appendix G.15)

From these Cp plots, it is found that increasing the angle of attack increases the difference in pressure co-efficient between the upper and lower aerofoil surface. At 15º angle of attack, the pressure co-efficient difference is more resulting in high lift co-efficient.

The flow separation point is found out for the entire angle of attack 5 º, 10º and 15º from the velocity vector plot. The line/rake is selected and a line on the aerofoil surface is created at the point where the reversed flow occurred, using the line tool option. The velocity along the x-direction is found out and the point at which the flow reverses is the flow separation point. The flow separation points for the different angle of attack are plotted as shown below.

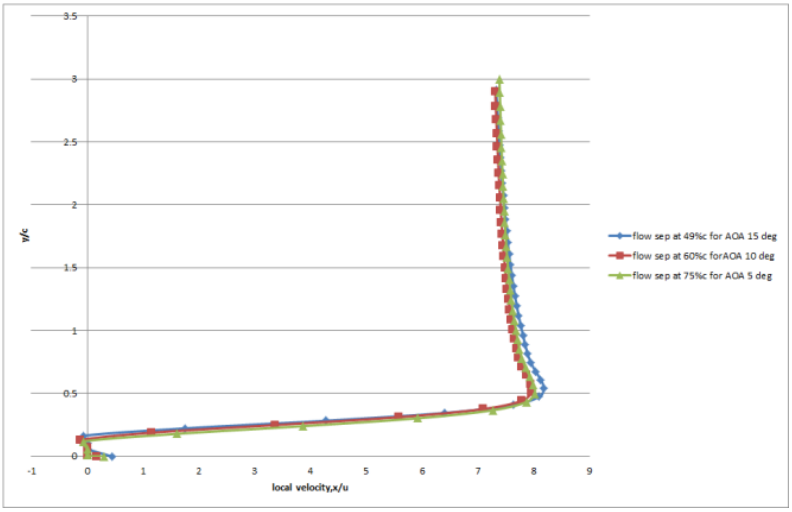

Figure 12: X-Velocity Vs Y/C Plot

The flow separation point for different angle of attack is found out from the velocity vector diagram. At 0º angle of attack, flow is not separated. At 5º angle of attack, flow separation occurs at 75% of chord. At 10º angle of attack, flow separation occurs at 60% of chord. At 15º angle of attack, flow separation occurs at 49% of chord. It is found that the flow separation point is delayed in corrugated dragonfly aerofoil compared to traditional streamlined NACA 0012 aerofoil. The flow separation point measured in the velocity vector plot is shown clearly in the below figure.

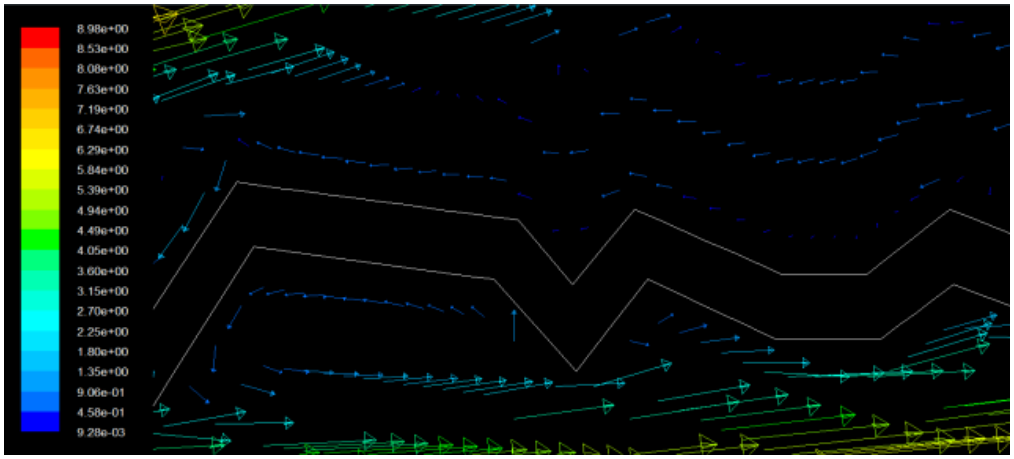

Figure 13: Flow Separation At 15º AOA

The aerodynamic performance such as lift co-efficient of the corrugated dragonfly aerofoil is compared with that of the NACA 0012 aerofoil at same Reynolds number. Also the lift co-efficient of corrugated dragonfly aerofoil at a Reynolds number of 34000 is taken from the base paper and is compared with the analysed corrugated dragonfly aerofoil at Reynolds number of 5×104.

The lift co-efficient values of NACA 0012 aerofoil for different angle of attack such as 0º, 5º, 10º and 15º obtained from the base paper are as follows

Table 1: CL Vs α For NACA 0012 Aerofoil at Re=50000

Angle of Attack (α)	**Lift co-efficient (C_L)**
0º	0
5º	0.387
10º	0.802
15º	0.905

Table 2: CL Vs α For Corrugated Dragonfly Aerofoil at Re=34000

Angle of Attack (α)	**Lift co-efficient (C_L)**
0º	0.12
5º	0.543
10º	1.082
15º	1.245

The lift co-efficient values of corrugated dragonfly aerofoil at a Reynolds number of 34000 for different angle of attack such as 0º, 5º, 10º and 15º obtained from the base paper are noted in the above table.

The lift co-efficient values of corrugated dragonfly aerofoil at a Reynolds number of 5×104 for different angle of attack such as 0º, 5º, 10º and 15º measured from the analysis results of FLUENT are tabulated as follows.

Table 3: CL Vs α For Corrugated Dragonfly Aerofoil at Re=50000

Angle of Attack (α)	**Lift co-efficient (C_L)**
0º	0.15
5º	0.587
10º	1.125
15º	1.296

The lift co-efficient result reveals that the corrugated dragonfly aerofoil at Reynolds number 5×104 has the highest performance compared to the other two. Thus corrugated dragonfly aerofoil can be highly used in micro air vehicles working at a low Reynolds number of 5×104 than the traditional streamlined aerofoil.

The below figure shows the comparison of the lift co-efficient for different angle of attacks for the corrugated dragonfly aerofoil and the traditional streamlined NACA 0012 aerofoil at same low Reynolds number of 50000. From this lift co-efficient plot, it is understood that corrugated dragonfly aerofoil is suitable for the low speed micro air vehicle applications. This improved aerodynamic performance of corrugated dragonfly aerofoil is due to the presence of corrugations which sustains an attached flow at low Reynolds number. The effect of vortices formation does not affect the aerodynamic performance at low speeds.

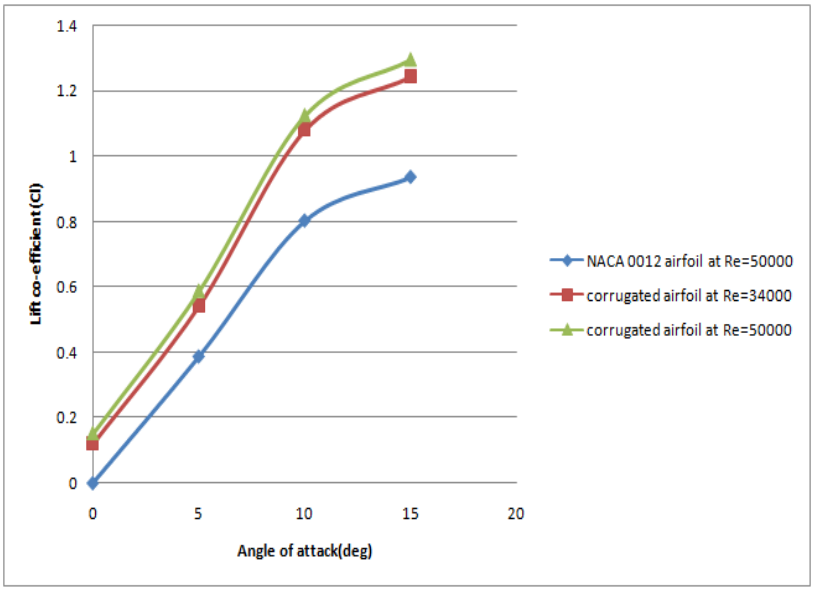

Figure 14: Lift Co-Efficient Vs Angle Of Attack Plot

Conclusion:

The corrugated dragonfly aerofoil is analysed at low Reynolds number of 50000 and the flow properties are obtained. The flow separation point is found out which is suppressed than that occurs in conventional streamlined aerofoil. Suppression of the flow separation point results in delaying of stall angle. The lift co-efficient measurement result shows the improved aerodynamic performance of the corrugated dragonfly aerofoil compared to that of traditional NACA 0012 aerofoil. This increased CL is due to the suppression of flow separation point caused due to the presence of corrugations. Therefore more lift is occurred for corrugated dragonfly aerofoil than for streamlined aerofoil at same angle of attack. Also the corrugated dragonfly aerofoil at Reynolds number of 34000 is compared in this study and the improvement of lift co-efficient is noted.

References:

1. Alain Pelletier and Thomas J. Mueller, ‘‘Low Reynolds Number Aerodynamics of Low-Aspect-Ratio, Thin/Flat/Cambered-Plate Wings’’, University of Notre Dame, Notre Dame, Indiana 46556, Journal of Aircraft, Vol. 37, No. 5, September–October 2000.
2. Alain Pelletier, “A Study of the Nonlinear Aerodynamic Characteristics of a Slender Double-Delta Wing in Roll.” Ph.D. Dissertation, The University of Notre Dame, April 1998.
3. Alexander D E 1984, ‘‘Unusual phase relationships between the forewing and hind wings in flying dragonflies’’, J. Exp. Biol. 109.
4. Anderson, John D., Jr., “Fundamentals of Aerodynamics”, 2nd ed. New York: McGraw-Hill, 1991.
5. Azuma A 1992, “The Biokinetics of Flying and Swimming (Berlin:Springer)”.
6. Azuma A and Watanabe T 1988, ‘‘Flight performance of a dragonfly’’ J. Exp. Biol. 137.
7. Brodsky A K 1994, ‘‘The aerodynamics of insect flight The Evolution of Insect Flight’’, New York, Oxford University Press.
8. Buckholz R H 1986, “The functional role of wing corrugations in living systems”, J. Fluids Eng. 108.
9. Carmichael, B. H. “Low Reynolds Number Airfoil Survey.” Volume I, NASA Contractor Report 165803, November 1981. DOI: 10.1016/S1001-6058(11)60262-X.
10. Ellington C P 1984a, “The aerodynamic of hovering insect flight: I”, The quasi-steady analysis Phil. Trans. R. Soc. 305.
11. Ennos A R 1989, ‘‘the effect on the optimal shapes of gliding insect and seeds’’, J. Zool. 219.
12. Hankin M A 1921, ‘‘the soaring flight of dragonflies’’, Proc. Camp. Phil. Soc. 20.
13. Jane Z, Wang, ‘‘Dissecting insect flight’’. Annu Rev Fluid Mech 2005.
14. Kesel A B 2000 Aerodynamic characteristics of dragonfly wing sections compared with technical aerofoil J. Exp. Biol.
15. Kesel, Antonia B. Aerodynamic characteristics of dragonfly wing sections compared with technical aerofoils. J Experiment Biol 2000.
16. KWOK R., MITTAL R. Experimental investigation of the aerodynamics of a modeled dragonfly wing section[C]. AIAA region I-MA student conference. Charlottesville, Virginia, 2005.
17. Laitone, E. V. “Aerodynamic Lift at Reynolds Numbers Below 7×104”, AIAA Journal, Vol. 34, No. 9, September 1996.

18. Lissaman, P. B. S., 1983, "Low-Reynolds-Number Airfoils," Annual Review of Fluid Mechanics, Vol. 15.
19. Miley, S. J. "An Analysis of the Design of Airfoil Sections for Low Reynolds Numbers", Ph.D. Dissertation, Mississippi State University, 1972.
20. Newman D J S and Wootton R J 1986 An approach to the mechanics of pleating in dragonfly wings J. Exp. Biol.
21. Newman, B. G., Savage, S. B., and Schouella, D., "Model Test on a Wing Section of an Aeschna Dragonfly," Scale Effects in Animal Locomotion, edited by T. J. Pedley, Academic Press, London, 1977.
22. Okamoto M, Yasuda K and Azuma A 1996, ''Aerodynamic characteristics of the wings and body of a dragonfly", J. Exp. Biol. 199.
23. Rees C J C 1975a Form and function in corrugated insect wings, Nature.
24. Rees C J C 1975b Aerodynamic properties of an insect wing section and a smooth aerofoil compared, Nature.
25. Rudolph R 1977 Aerodynamic properties of Libellula quadrimaculata L. (Anisoptera: Libelludidea), and the flow around smooth and corrugated wing section models during gliding flight, Odonatologica.
26. Rüppel, G. (1989), ''Kinematic analysis of symmetrical flight manoeuvres of Odonata'', J. Exp. Biol. 144.
27. Savage S B, Newman B G and Wong D T M 1979, ''The role of vortices and unsteady effects during the hovering flight of dragonflies'', J. Exp. Biol. 83.
28. SHI Sheng-xian, LIU Ying-zheng, CHEN Jian-min, ''An Experimental Study Of Flow Around A Bio-Inspired Airfoil At Reynolds Number 2.0×103'', Shanghai Jiao Tong University, Shanghai 200240, Journal of hydrodynamics, 2012,24(3):410-419
29. Somps C and Luttges M 1985, ''Dragonfly flight: novel uses of unsteady separated flow'', Science 228.
30. Tamai M, Zhijian Wang, Ganesh Rajagopalan, Hui Hu, 2007, ''Aerodynamic Performance of a Corrugated Dragonfly Airfoil Compared with Smooth Airfoils at Low Reynolds Numbers'', In 45th AIAA Aerospace Sciences Meeting and Exhibit, Reno, Nevada, Jan.
31. Tamai, M., "Experimental investigations on biologically inspired airfoils for MAV applications", Master thesis, Aerospace Engineering Department, Iowa State University, Nov., 2007.
32. Thomas A L R, Taylor G K, Srygley R B, Nudds R L and Bomphrey R J 2004, ''Dragonfly flight: free-flight and tethered flow visualization reveal a diverse array of unsteady lift-generation mechanisms, controlled primarily via angle of attack'', J. Exp. Biol. 207.
33. Thomas J. Mueller, ''Aerodynamic Measurements at Low Reynolds Numbers for Fixed Wing Micro-Air Vehicles'', University of Notre Dame Notre Dame, IN 46556, September 13-17, 1999, VKI, Belgium.
34. Usherhood, J.R., Ellington, C.P., 2002a. ''The aerodynamics of revolving wings, I. Model hawkmoth wings''. J. Exp. Biol. 205.
35. Vargas A 2006, "Numerical investigation of the aerodynamic characteristics of a dragonfly wing section", PhD Dissertation, The George Washington University.
36. Vargas, A., and Mittal, R., "Aerodynamic Performance of Biological Airfoils," 2nd AIAA Flow Control Conference, Portland, OR, AIAA Paper 2004-2319, 2004.
37. Vogel S 1957, ''Flight in drosophila: III. Aerodynamic characteristics of fly wing and wing models'', J. Exp. Biol. 46.
38. Wakeling, J. M. and Ellington, C. P. (1997). ''Dragonfly flight. I. Gliding flight and steady-state aerodynamic forces'', J. Exp. Biol.200.
39. Wang,Z.J.,2004. ''The role of drag in insect hovering''. The Journal of Experimental Biology, 207.
40. Wootton R J and Kukalova-Peck J 2000, ''Flight adaptations in Palaeozoic Palaeoptera (Insecta)'', Biol. Rev. 75.
41. W. Shyy, Y. Lian, J. Tang, D. Viieru, H. Liu, "Aerodynamics of Low Reynolds Number Flyers", Cambridge University Press, UK, 2008.